Mediterranean Arhaeology and Archaeometry, Vol. 12, No 2, pp.193-211

COMPOSITION, PRESERVATION AND PRODUCTION TECHNOLOGY OF AUGUSTA EMERITA ROMAN GLASSES FROM THE FIRST TO THE SIXTH CENTURY AD

Teresa Palomar[a]*, Manuel Garcia-Heras[a], Rafael Sabio[b], Jesus-Maria Rincon[c] & Maria-Angeles Villegas[a]

[a] Instituto de Historia, Centro de Ciencias Humanas y Sociales, CSIC, Calle Albasanz, 26-28, 28037 Madrid, Spain.
[b] Museo Nacional de Arte Romano, Calle José Ramón Mélida, s/n, 06800 Mérida, Spain.
[c] Instituto Eduardo Torroja de Ciencias de la Construcción, CSIC, Calle Serrano Galvache, 4, 28033 Madrid, Spain.

Received: 24/10/2011
Accepted: 23/01/2012
Corresponding author: Teresa Palomar (teresa.palomar@cchs.csic.es)

ABSTRACT

This paper presents the results derived from an archaeometric study undertaken on glass samples from the Roman town of Augusta Emerita (Mérida, Spain). The main goal of the research was to provide for the first time some compositional and technological insights into the glass finds unearthed in this town. Glass samples from different sites and chronology, either from inside or from outside the perimeter of the ancient town and from the first to the sixth century AD, were analyzed and characterized through optical microscopy (OM), scanning electron microscopy (SEM), energy dispersive X-ray microanalysis (EDS), X-ray fluorescence (XRF) spectrometry and VIS spectrophotometry. Resulting data indicated that all the samples studied were natron-based soda lime silicate glasses, even though two chronological and compositionally distinct groups were distinguished. One composed of Early Empire glasses and a second one composed of glasses from the fourth century AD onward, which was characterized by the presence of the so-called HIMT (high iron, manganese, and titanium) glasses. Comparison with coeval glasses suggested that Augusta Emerita shared the same trade glass circles than other contemporary Roman towns, within the frame of a secondary production scale. Finally, some outstanding differences connected to composition and chronology were found, since Late Roman glasses presented a higher and distinct degree of alteration than Early Empire ones.

KEYWORDS: Roman glass, Augusta Emerita, Archaeometry, Chemical composition, Degradation

1. INTRODUCTION

1.1. Previous considerations and research aims

Roman glass items have been mainly found in domestic and funerary contexts. Above all Romans used glass to produce hollow vessels, even though mosaic tiles and flat window glass were also produced to a lesser extent. In the Republican period, glass was a minor craft and, consequently, an expensive product of a marked Hellenistic influence. Roman Republican glass was generally cast formed and strongly coloured. However, the most important technical development took place during the first decades of the Empire with the introduction of the glassblowing technique. Glassblowing signified a true revolution since it allows the production of vessels with thinner walls and a wider variety of shapes, the production is quicker and uses a lower amount of glass, and production costs are dramatically reduced. These latter aspects meant that glass reached more segments of the Roman society, which produced a change in its high status value to be transformed into an everyday functional material (Stern, 1999, Fleming, 1999).

Roman glass production reached the highest splendour in the first half of the second century AD when a wide range of glass objects of any kind was being produced. Glass containers and types varied with fashions but the technology remained unchanged for many centuries. In addition, from the late second and during the third century AD fashion styles became increasingly regionalized and quality progressively decays. Glass workshops settled in Rome, Campania and the Po valley from the beginning of the era. With the expansion of the Empire other glass workshops were established throughout trade routes, such as the Rhineland sites (Wedepohl and Baumann, 2000). From the mid to the late first millennium AD in the eastern Mediterranean region, the raw glass production was centered around a relatively small number of workshops, some of them located in Israel (the Levantine I and Levantine II compositional groups) and others still unknown, such as the workshops which elaborate the so-called HIMT glass-High Iron Manganese Titanium, where glass was produced on a large scale and then broken and traded into chunks. (Freestone, 2006, Freestone *et al.*, 2002, Freestone, 1994). There is only limited evidence for local glass making, probably as a secondary production scale (Jackson *et al.*, 1998).

The recycling of broken glass was an important part of the Roman glass industry (Allen, 1998). In the Western Roman Empire there is evidence that recycling of glass was frequent and extensive and that broken glassware was concentrated at local sites prior to re-melting into raw glass (Jackson *et al.*, 1998). Chemical composition variations due to recycling could be evaluated by means of the high percentages of some elements used as colouring agents (Freestone, 2005).

Glass has been widely found in Roman archaeological sites where it normally appears very fragmented. This fact very often makes extremely difficult to assign a glass fragment to a given typology. Chemical-physical characterization techniques have been used to get information on technology and raw materials employed in glass production. Most analytical works have been concentrated on set of samples coming from a given localization and chronology (Paynter, 2006, Arletti *et al.*, 2008). However, there are very few works which were focused on technological evolution of glasses of different chronology (Silvestri *et al.*, 2005).

The development of glass in the Iberian Peninsula was similar to that of other areas of the Western Roman Empire. During the first centuries of our era the arrival of glass makers and high quality raw materials supposed the growing of the glass

production (Vigil Pascual, 1969). After the fall of the Western Roman Empire trade relationships were collapsed and, consequently, the access to good raw materials came to an end. The employment of low quality raw materials and the reusing (remelting) of glasses introduced an important amount of impurities, which resulted in low quality and darker glasses.

In the main Roman towns of the Iberian Peninsula, such as Caesaraugusta, Tarraco, Augusta Emerita and so on, a wide variety of glasses in relation to typology, colours, and forming techniques are well known. Nevertheless, up to now, very few ensembles have been studied from an archaeometric perspective. These studies have been concentrated on coastal sites (Ramón Peris, 2002-2003, Dominguez-Bella and Jurado-Fresnadillo, 2004, Domenech-Carbo *et al.*, 2006, Garcia-Heras *et al.*, 2007) and settlements located in the main communication and trade routes (Rincón, 1984, Gómez-Tubío *et al.*, 2006, Carmona *et al.*, 2008).

The best-documented glass ensemble from Augusta Emerita is that dated to the Early Empire period. Among the different types, tableware containers, bottles, stirring rods, and so on can be highlighted (Caldera de Castro, 1983). On the other hand, only three glass fragments from this ensemble have been previously studied by chemical-physical techniques (Rincón, 1984). For this reason, the main goal of this research was to provide for the first time some compositional and technological insights into the glass finds unearthed in the Roman town of Augusta Emerita. To undertake such a research glass samples from different sites and chronology, either from inside or from outside the perimeter of the ancient town and from the first to the sixth century AD, were archaeometrically characterized. Degradation pathologies of glasses were also studied with the aim to establish probable corrosion mechanisms occurred and to assess their current state of preservation.

1.2. Archaeological background

Augusta Emerita is located in the southwestern area of the Iberian Peninsula and lies under the modern city of Mérida, which nowadays belongs to the administrative province of Badajoz. It was founded in 25 BC and was one of the most important towns of the Roman Empire in the Iberian Peninsula. The site was the head capital of the Roman administrative province of Lusitania. Notable routes of communication set off from this town such as the so-called *Vía de la Plata* (the Silver Way), which joined Augusta Emerita with Asturica Augusta, located in the nowadays town of Astorga within the current administrative province of León.

The glass fragments studied come mostly from different sites within the perimeter of the ancient Roman town (Fig. 1). The samples M-1 and M-2 come from the Amphitheater House and were found under a mosaic pavement (Tab. I). Both

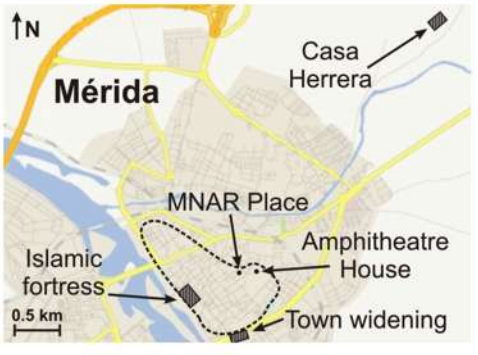

Figure 1. Location of the sampling sites within the perimeter of the ancient Roman town and its surroundings. The dashed line points out the Roman wall of the town.

samples were dated from the first to the second century AD, which was the date estimated for the building of the house (García Sandoval, 1966). The sample M-1 can be assigned to an Isings 41a shape (Isings, 1957) and is 70 mm in base diameter and 35 mm in height.

Three glass fragments (samples M-3, M-4, and M-5) come from the place in which the nowadays National Museum of Roman Art at Mérida was built (Tab. I). The site was located in the surroundings of the ancient Roman town and was used as a dump place. For this reason the items found here showed a wide variety and chronology. These three glass fragments were dated into

Tab. I. Main characteristics of the glass samples studied.

Sample	Site	Chronology	Forming technique	Colour
M-1	Amphitheatre House	1st-2nd cent AD	Mould (Isings 41 a)	Emerald green
M-2	Amphitheatre House	1st-2nd cent AD	Mould	Emerald green
M-3	MNAR site[a]	1st-3rd cent AD	Flat	Light grey
M-4	MNAR site[a]	1st-3rd cent AD	Flat	Yellowish
M-5	MNAR site[a]	1st-3rd cent AD	Mosaic	Yellowish
M-6	Islamic fortress	1st-3rd cent AD	Mould	Light blue
M-7	Islamic fortress	1st-3rd cent AD	Blown	Yellowish
M-8	Islamic fortress	1st-3rd cent AD	Flat	Greenish
M-9	Islamic fortress	1st-3rd cent AD	Melt waste	Greenish
M-10	Town widening	4th cent AD	Melt waste	Olive green
M-11	Town widening	4th cent AD	Melt waste	Olive green
M-12	Casa Herrera	4th-6th cent AD	Unknown (Possibly blown)	Olive green
M-13	Casa Herrera	4th-6th cent AD	Unknown (Possibly mould)	Olive green

[a] MNAR: National Museum of Roman Art (Mérida, Spain)

a general Early Empire date.

The Islamic fortress located beside the river Guadiana was built in the ninth century AD on a former area of the Roman town close to the Roman bridge. This area was occupied, among other elements, by an ancient gate and thermal bath buildings dated in Imperial times as some archaeological excavations have revealed. The glass fragments of the samples M-6, M-7, M-8, and M-9 were found in a corridor located between the wall and the dyke of the former Roman town (Tab. I). This site seems to be also used as a dump place in Roman imperial times.

The zone of the modern town widening was excavated in 1948. Evidences of industrial activities, such as probable blow canes and melt wastes, were found in this area, which suggested the location of a possible glass workshop. Glass samples M-10 and M-11 belongs to some of these melt wastes (Tab. I). The association of these glasses with other materials dated the settlement in the fourth century AD (Lang and Price, 1975).

Finally, two glass fragments (samples M-12 and M-13) come from the basilica of Casa Herrera, which is a site located outside the perimeter at approximately 6 km from the ancient Roman town of Augusta Emerita. The sample M-12 was located in a grave, while the sample M-13 was unearthed in an external room of the basilica. Either the architecture or the decorative sculpture dated the site between the fourth and fifth centuries AD, even though some finds could rise the beginning of the sixth century AD (Caballero Zoreda and Ulbert, 1976).

2. EXPERIMENTAL

2.1. Description of samples

A set of 13 glass samples were analyzed. Samples were selected with the aim of obtaining the widest variety of representative materials (Tab. I, Fig. 2). They come from five different sites, namely the Amphitheater House, the place in which the National Museum of Roman Art is currently located, the Islamic fortress foundation, the zone of the modern town widening, and the basilica of Casa Herrera. Chronology of glass samples is comprised from the first to the sixth century AD. As far as forming techniques are concerned, samples selected mostly corresponded to flat and mould blown glass and one of them (sample M-5) to a mosaic glass. This latter, from its curvature, could be attributed to a full piece of approximately 80 mm in diameter. Colour of samples was emerald green, light blue, light grey, and yellowish green. All the glasses studied were deposited in the grounds of the National Museum of Roman Art.

2.2. Characterization techniques

The glass samples studied were characterized by the following techniques: optical microscopy (OM), scanning electron microscopy (SEM), energy dispersive X-ray microanalysis (EDS), X-ray fluorescence (XRF) spectrometry and VIS spectrophotometry.

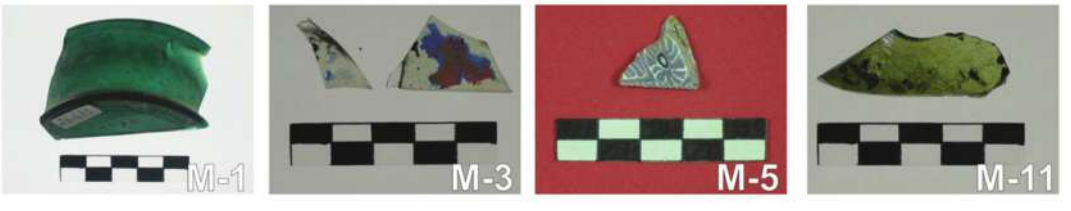

Figure 2. Images of the samples as-received in the laboratory. Transmitted (M-1, M-3, and M-11) and reflected light (M-5).

OM was carried out by a Leica MZ16 reflected light microscope equipped with a Leica DC300 camera. SEM observations were undertaken by a Hitachi S-3400-N electron microscope (CCHS-CSIC), using acceleration voltages of 15 kV and the secondary electrons mode. Samples were examined and EDS micro-analyzed on both surface and resin inlayed polished cross-section, using a carbon conductive coating deposited through a sputter coater Polaron SC7620. The sample M-5 was the only one not coated and was observed using the backscattered electrons mode (BSE). EDS micro-analyses were accomplished by a Bruker AXS XFlash Quantax 4010 spectrometer with energy resolution of 125 eV (Mn Kα) attached to the SEM equipment. EDS determinations with the theoretical inner pattern were obtained by using the ZAF method of correction and the Bruker Sprit 1.8 analytical software.

Semi-quantitative chemical analysis by XRF was carried out by a PANalytical Axios wavelength dispersed X-ray spectrometer equipped with a tube of rhodium of 4 kW and 60 kV. Analytical determinations were undertaken through the standard-less analytical software IQ+ (PANalytical) based on fundamental parameters from synthetic oxides and well-characterized natural minerals. In addition, Sheffield glass nos. 7 and 10 (Society of Glass Technology) are commonly used as internal routine control standards. Powder samples (1 g approx.) for bulk XRF analysis were prepared by grinding body glass fragments, with their most external surfaces removed by polishing, in an agate mortar. After that, pressed boric acid pellets were made, using a mixture of n-butylmethacrylate and acetone (10:90 wt %) as binding medium.

All the samples were analyzed by XRF except glass fragments M-7, M-12, and M-13. These samples were micro-analyzed by EDS on polished cross-sections, since they did not present enough size to be analyzed by XRF. The bulk of the sample M-5 could not be analyzed since it is a very valuable glass item and it could not be micro-destroyed following cataloguing rules of the Museum.

The colour of the glass samples was determined by visible spectrophotometry (VIS) with an Ocean Optics HR 4000 CG spectrophotometer. Spectra were recorded in the 250-1100 nm range on glass samples of approximately 1 mm thick obtained by polishing both sides of the samples to optical quality.

3. RESULTS

3.1. Chemical composition of glasses

Chemical data showed that all the samples were natron-based soda lime silicate glasses, even though they presented compositional differences (Tab. II). Fig. 3a displays chemical composition in a ternary plot in which the majority of glasses were concentrated into a single group around 66 wt % of SiO_2, 17 wt % of [Na_2O + K_2O] and 12 wt % of [MgO + CaO + Al_2O_3]. The glass fragments M-12 and M-13 from the Casa Herrera site presented a slight deviation towards lower contents of SiO_2 and higher concentrations of Na_2O.

The chemical composition of Roman glasses from other locales of the Iberian Peninsula (Carmona *et al.*, 2008, Dominguez-Bella and Jurado-Fresnadillo, 2004, Ramón Peris, 2002-2003, Domenech-Carbo *et al.*, 2006, Garcia-Heras *et al.*, 2007, Gómez-Tubío *et al.*, 2006, Rincón, 1984) were plotted in two ternary plots: the first one for Early Empire glasses (Fig. 3b) and the second one for Late Roman glasses dated from the fourth century AD onward (Fig. 3c). Resulting plots exhibited a quite similar pattern than that for Augusta Emerita samples. Early Empire glasses were associated to the group mentioned above, except some glasses from Partida de Mura (Liria, Valencia), which presented SiO_2 contents close to 74 wt % (Domenech-Carbo *et al.*, 2006), one glass from Dehesa de la

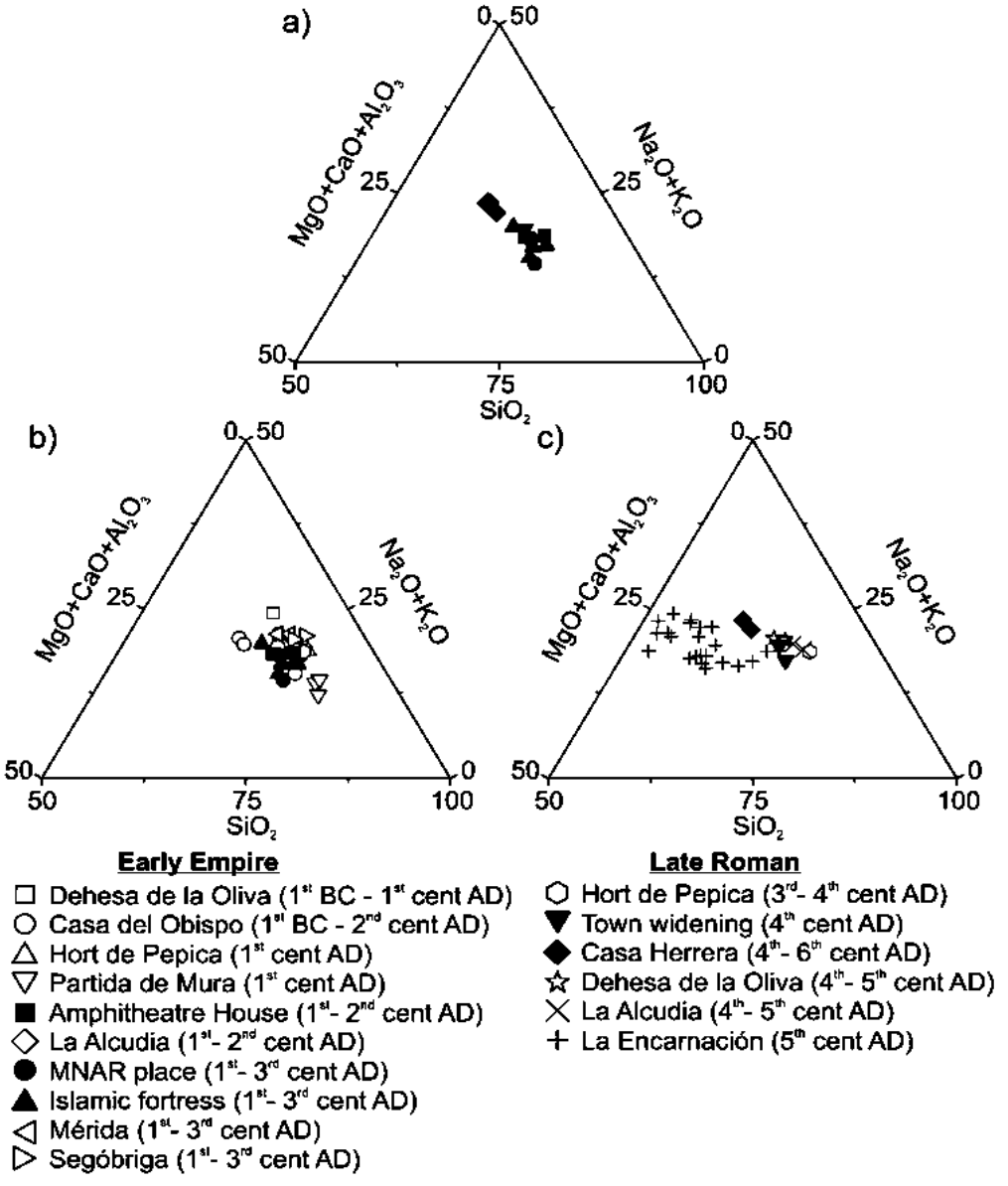

Figure 3. Ternary plots of the main chemical components of glasses (wt %). a) Roman glass samples from Augusta Emerita. b) Early Empire glass samples from the Iberian Peninsula including those from Augusta Emerita. c) Late Roman glass samples from the Iberian Peninsula including those from Augusta Emerita. Shaded symbols: samples from Augusta Emerita. References: Dehesa de la Oliva (Madrid) (Carmona *et al.*, 2008). Casa del Obispo (Cádiz) (Dominguez-Bella and Jurado-Fresnadillo, 2004). Hort de Pepica (Valencia) (Ramón Peris, 2002-2003). Partida de Mura (Valencia) (Domenech-Carbo *et al.*, 2006). La Alcudia (Alicante) (Garcia-Heras *et al.*, 2007). Mérida (Badajoz) (Rincón, 1984). Segóbriga (Cuenca) (Rincón, 1984) and La Encarnación (Sevilla) (Gómez-Tubío *et al.*, 2006).

Oliva (Patones, Madrid) with a 22.51 wt % content of Na_2O (Carmona *et al.*, 2008), and two glass fragments from Casa del Obispo (Cádiz) which presented a concentration of MgO close to 4 wt % (Dominguez-Bella and Jurado-Fresnadillo, 2004). In the case of glasses from Partida de Mura, the high content of SiO_2 could be due to weathering since the SiO_2 contents reported barely showed differences between core and corroded parts of the glasses. On the other hand, either the glass from Dehesa de la Oliva or the two fragments from Casa del Obispo are associated to a wide chronology which also encompasses the first century BC. In all probability it deals with glasses from an early chronology and, therefore, from other sources as the high MgO content might suggest. The chemical composition of Late Roman glasses displayed, on the contrary, a higher variability (Fig. 3c). Although some of them presented close compositions to Early Empire glasses, they also showed a higher dispersion due, to a great extent, to the low SiO_2 concentrations of glasses from La Encarnación (Sevilla). Fig. 4 shows a map of the Roman Iberian Peninsula with the location of the sites from which glasses came.(see relevant results from 1st-2nd AD Roman Patras, Greece, in Liritzis *et al.*, 1997).

In the case of emerald green fragments M-1 and M-2, a high concentration of CuO (4.2 wt %) and a small percentage of SnO_2 (~0.2 wt %) were detected. Their incorporation could be through the addition of bronze metal shavings (94 Cu: 6 Sn) to the glass. According to Fleming (1999) the common procedure for deep green colour in Roman glasses consisted of adding lead to a green glass obtained from copper. This can be explained by the shift of the absorption band of Cu^{2+}-ions towards higher wavelengths due to the incorporation of lead oxide, which provides a more basic glass network (Carmona *et al.*,

Figure 4. A map of the Roman Iberian Peninsula with its *conventus* showing the location of the sites from which glass samples of Fig. 3b and c came.

2009). Nevertheless, in the case of M-1 and M-2 glasses, only a low percentage of lead oxide (~0.1 wt %) was detected by XRF. This indicates that a final dark green colour was also achieved with a high content of CuO in its oxidized form and without the addition of lead, as is discussed in the next section.

3.2. Analysis of chromophores

Except in samples M-12 and M-13 due to their small size and in sample M-5 which could not be micro-destroyed, the chromophores of all the glasses were determined. They presented four distinct colourings: emerald green, light blue, light grey, and different shades of yellowish green (Tab. I).

The emerald green colour of samples M-1 and M-2 is related to the presence of the band at 776 nm assigned to Cu^{2+}-ions (Fig. 5a). The intensity and width of this band is attributed to the high content of CuO in the glass bulk (Tab. II). However, the presence of other chromophores, whose absorption bands can be overlapped due to the very wide band, can not be discarded.

The spectroscopic analyses carried out demonstrated that all the glasses presented some of the bands corresponding to the Fe^{2+}/Fe^{3+} ions (Fig. 5a, b, c, d). The colour of the glass will depend on both the redox balance and the relative concentrations of ferric and ferrous ions (Férnandez Navarro, 2003). The fragment M-6 presented the bands of both ions. The Fe^{3+}-ion triplet at 375, 421, and 446 nm respectively, was overlapped due to the intensity of the band corresponding to the Fe^{2+}-ion at 1031 nm

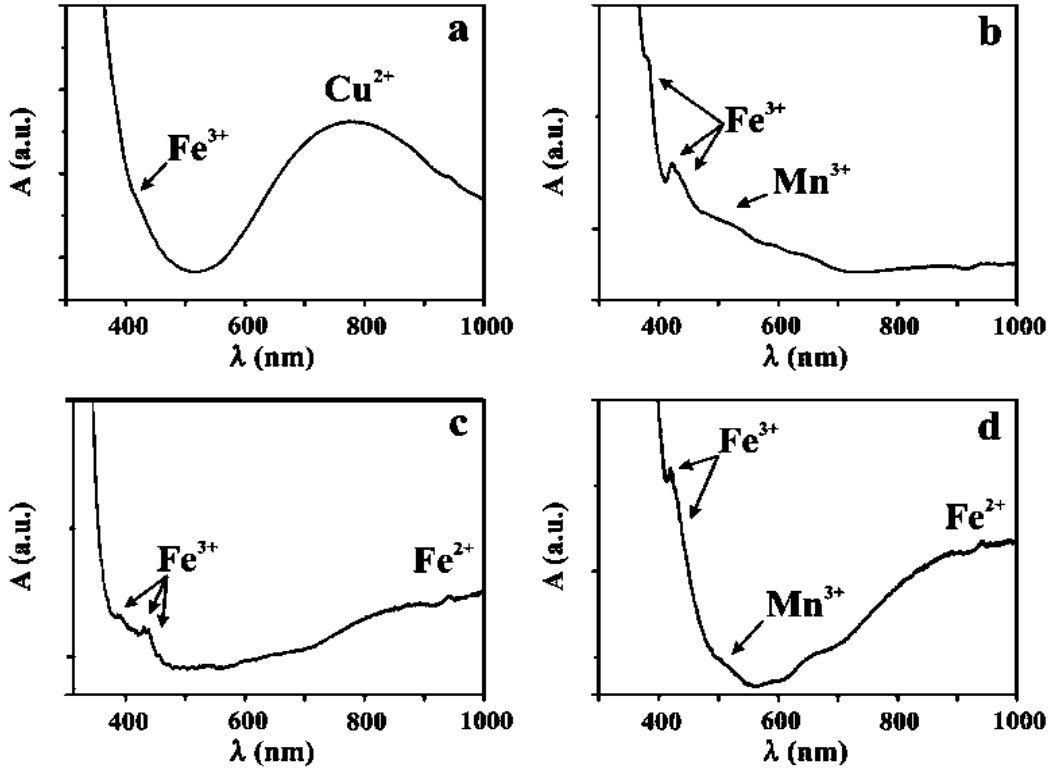

Figure 5. UV-VIS-NIR spectra from glass samples. a) Sample M-1, emerald green. b) Sample M-3, light grey. c) Sample M-6, light blue. d) Sample M-11, olive green.

Table II. Results of bulk chemical analyses by XRF and EDS (wt %).

Comp.	Samples											
	M-1 (1^{st}-2^{nd} ce AD) XRF	M-2 (1^{st}-2^{nd} ce AD) XRF	M-3 (1^{st}-3^{rd} ce AD) XRF	M-4 (1^{st}-3^{rd} ce AD) XRF	M-6 (1^{st}-3^{rd} ce AD) XRF	M-7 (1^{st}-3^{rd} ce AD) EDS	M-8 (1^{st}-3^{rd} ce AD) XRF	M-9 (1^{st}-3^{rd} ce AD) XRF	M-10 (4^{th} ce AD) XRF	M-11 (4^{th} ce AD) XRF	M-12 (4^{th}-6^{th} ce AD) EDS	M-13 (4^{th}-6^{th} ce AD) EDS
Na_2O	15.30	15.88	16.72	13.27	15.71	17.9	14.22	15.95	15.38	17.84	21.4	19.3
MgO	1.24	0.98	0.66	0.54	0.54	0.5	0.40	0.55	1.00	0.96	1.3	0.8
Al_2O_3	2.37	1.65	2.20	2.50	2.62	2.4	2.46	2.08	2.26	2.72	3.4	2.6
SiO_2	62.08	65.22	66.47	69.07	68.43	62.5	67.69	69.85	64.03	63.15	59.0	59.4
P_2O_5	0.41	0.40	0.23	0.15	0.14	--	0.19	0.28	0.07	0.13	0.1	--
SO_2	0.30	0.17	0.18	0.14	0.13	0.1	0.13	0.14	0.19	0.21	0.4	0.2
Cl^-	1.00	1.21	0.98	0.96	1.09	1.1	1.10	1.05	0.91	0.86	0.9	0.9
K_2O	1.26	1.11	0.70	0.57	0.72	0.8	0.54	0.73	0.48	0.44	1.0	1.3
CaO	8.00	6.72	8.74	9.99	9.01	9.7	10.13	7.74	8.10	7.58	9.4	10.1
TiO_2	0.33	0.15	0.12	0.09	0.10	0.6	0.09	0.06	0.67	0.64	0.7	--
MnO	1.28	0.66	1.87	2.08	0.46	2.6	2.41	0.75	3.38	2.71	1.1	2.0
Fe_2O_3	1.80	1.18	0.87	0.54	0.73	1.9	0.49	0.61	3.39	2.57	1.3	3.3
CuO	4.16	4.18	--	--	0.16	--	--	--	--	0.03	--	--
SrO	0.08	0.06	0.08	0.09	0.06	--	0.09	0.07	0.08	0.08	--	--
SnO_2	0.17	0.33	--	--	--	--	--	--	--	--	--	--
Sb_2O_3	0.03	--	0.14	--	0.03	--	--	0.10	--	--	--	--
BaO	--	0.04	--	--	--	--	0.05	--	0.05	0.08	--	--
PbO	0.17	0.05	0.03	--	0.07	--	--	--	--	--	--	--

-- Not detected

Note: Shaded columns indicate the different sites of the samples (Tab. I).

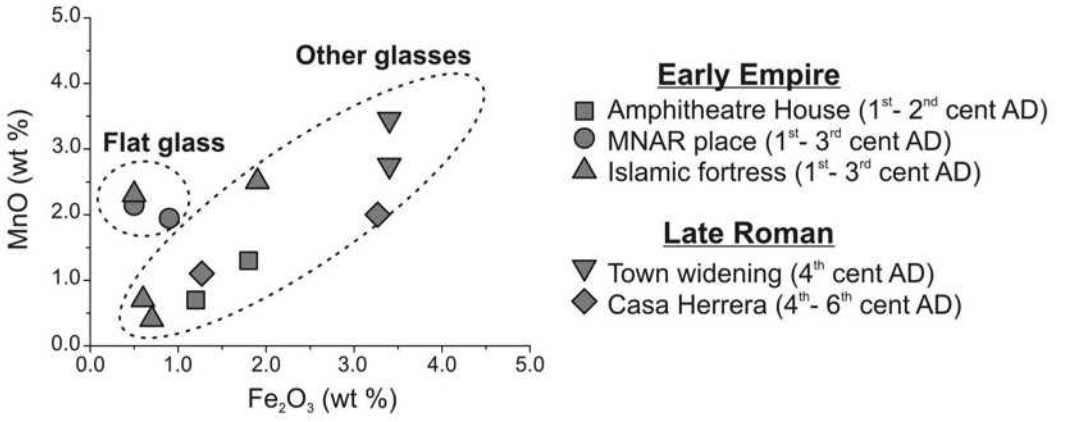

Figure 6. Binary plot of Fe_2O_3 vs. MnO (wt %) contents for the analyzed glasses.

(Fig. 5c), which results in a blue colour glass.

The light grey glass sample M-3 presented the bands corresponding to the Fe^{3+}-ions at 379, 419, and 436 nm respectively; and to the Mn^{3+}-ions at 508 nm (Fig. 5b). The addition of low percentage of manganese oxide chromatically compensates the greenish colouring due to the Fe^{2+}/Fe^{3+} ions, thereby giving rise to an almost colourless glass [Reaction (1)]. On the contrary, if glass presents high concentrations of both manganese and iron oxides, the predominant colour will be brown yellowish as is the case of the M-11 fragment. The visible spectrum of this sample presented the bands of Fe^{3+}-ions (at 419 and 435 nm respectively), Mn^{3+}-ions (at 513 nm), and Fe^{2+}-ions (at 1020 nm) (Fig. 5d).

$$4MnO_2 \rightarrow 2Mn_2O_3 + O_2 \ (> 600^{o}\ C)$$

$$Mn_2O_3\ (violet) + 2FeO\ (blue) \rightarrow 2MnO + Fe_2O_3\ (yellow) \quad (1)$$

The binary plot of Fig. 6 displays concentration data of Fe_2O_3 vs. MnO (wt %) for the samples studied. Apart from the clear separation of glasses dated from the fourth century AD onward which will be discussed later, the flat glass samples (M-3, M-4, and M-8, probably window glasses) exhibited a higher content of the manganese oxide than that of the iron oxide. This indicated that manganese oxide was probably added with the aim to eliminate the residual colouring provided by iron ions and, therefore, giving rise to an almost colourless glass.

3.3. Surface decorations

The sample M-5 was the only glass sample which presented a decoration on its surface. It deals with a mosaic glass which shows black and white colour circular motifs on a lightly yellow base glass (Fig. 2).

Five different areas of the surface were micro-analyzed by SEM-BSE-EDS (Fig. 7a). The lightly yellow base glass was a soda lime silicate glass which presented a surface dealkalinization layer (Fig. 7a, analysis M-5 A1 and A2). As a consequence of leaching and loss of alkaline oxides, some other elements such as Al_2O_3 resulted relatively enriched. However, alumina can be associated to impurities of the sand and, consequently, it could be particularly diagnostic of a different silica sand source for this glass fragment in comparison with the rest of the glasses here analyzed. Black decoration motifs were composed of small aggregates of manganese oxide (Fig. 7a, analysis M-5 A3; Fig. 7b). In addition, it was verified that white decoration motifs crossed completely the fragment and presented the same design in both sides of

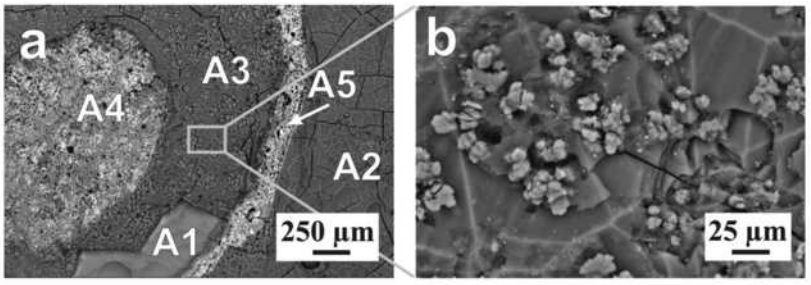

Analyses	Na_2O	MgO	Al_2O_3	SiO_2	P_2O_5	SO_2	Cl^-	K_2O	CaO	TiO_2	MnO	Fe_2O_3	Sb_2O_3
M-5 A1 (a)	10.2	0.5	3.4	70.9	--	0.4	1.0	1.1	9.3	--	2,3	0.8	--
M-5 A2 (a)	1.5	2.4	15.8	71.1	--	--	0.3	5.5	2.7	--	--	0.7	--
M-5 A3 (a)	1.8	2.8	15.1	64.7	0.3	0.4	0.3	5.5	3.4	0.5	4.2	1.1	--
M-5 A4 (a)	1.8	2.3	12.7	48.6	0.4	--	0.2	3.5	11.0	--	1.3	1.3	16.7
M-5 A5 (a)	1.9	2.3	11.0	42.4	0.6	--	0.2	2.6	12.2	--	3.9	2.0	20.9

Figure 7. SEM-BSE micrographs from the surface of glass sample M-5. a) Detail of the decoration with black (A3) and white (A4 and A5) circular motifs. The light yellow base glass corresponds to A1 and A2 areas. b) Small aggregates of manganese oxides in the black decoration. The table attached shows average results from EDS microanalyses (wt %). -- Not detected.

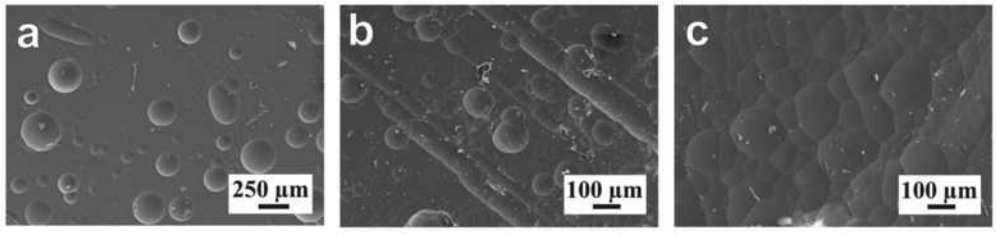

Analyses	Na_2O	MgO	Al_2O_3	SiO_2	P_2O_5	SO_2	Cl^-	K_2O	CaO	TiO_2	MnO	Fe_2O_3	CuO
M-12 (a)	11.4	2.2	4.4	65.8	0.3	0.5	0.8	1.1	8.9	0.6	1.5	2.6	--
M-4 (b)	15.0	0.8	3.1	64.5	0.1	0.1	0.9	0.9	11.2	0.6	1.9	0.9	--
M-6 (c)	12.9	0.4	3.0	67.9	--	0.1	0.7	1.2	11.3	0.2	0.6	0.9	0.7

Figure 8. SEM micrographs of surface craters. a) Glass sample M-12. b) Glass sample M-4. c) Glass sample M-6. The table attached shows average results from EDS microanalyses (wt %). -- Not detected.

the glass. These white areas showed high concentrations of Sb_2O_3 (Fig. 7a, analysis M-5 A4 and A5). According to Fleming (1999), the addition of antimony minerals, such as stibnite, causes the reaction of antimony with CaO in the glass matrix leading with the precipitation of micro-crystals of calcium antimonite responsible for the white opaque appearance.

3.4. State of preservation

The glass samples studied presented different degradation pathologies, such as craters, dealkalinization layers, brown aggregates, and interlaminated dark deposits.

Craters were observed on surfaces of all the glasses. They showed three different morphologies: craters isolated (Fig. 8a), craters isolated and lengthened in shape (Fig. 8b), and craters distributed in an interconnected network (Fig 8c). The size of the circular craters, isolated or interconnected, varied from 100 to 250 µm.

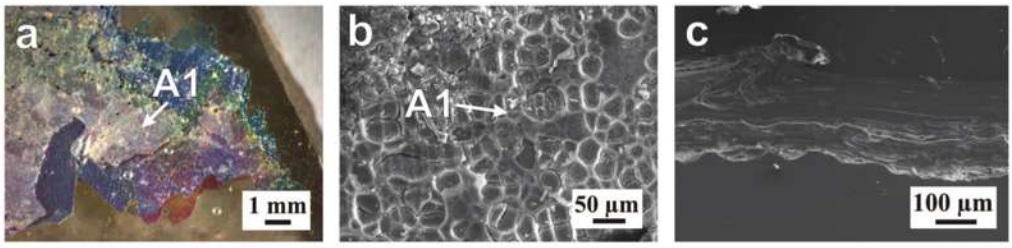

Analyses	Na_2O	MgO	Al_2O_3	SiO_2	P_2O_5	SO_2	Cl^-	K_2O	CaO	Fe_2O_3
M-3 A1 (a)	0.9	1.2	14.0	74.2	--	0.2	0.2	5.2	3.1	0.9
M-6 A1 (b)	0.8	1.7	16.8	67.4	0.5	--	--	7.3	3.9	1.6

Figure 9. Images from different samples. a) Binocular microscope image of iridescent layers from glass sample M-3. b) SEM micrograph of the irregular iridescent layer from glass sample M-6. c) SEM micrograph in cross-section of the iridescent layer from glass sample M-9. The table attached

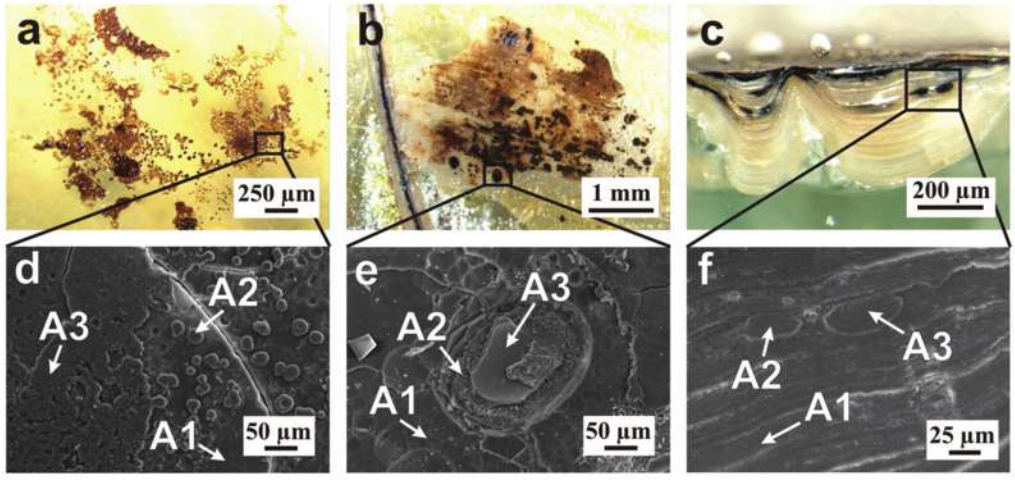

Analyses	Na_2O	MgO	Al_2O_3	SiO_2	P_2O_5	SO_2	Cl^-	K_2O	CaO	TiO_2	MnO	Fe_2O_3	Sb_2O_3	PbO
M-10 A1 (d)	5.1	1.1	14.8	62.1	0.4	0.2	0.3	0.9	8.0	1.2	1.1	4.8	--	--
M-10 A2 (d)	1.3	0.6	7.6	27.5	0.2	--	0.6	0.8	20.2	4.9	20.4	15.2	--	0.5
M-10 A3 (d)	1.8	0.8	9.2	34.9	0.6	--	0.7	0.6	13.7	5.4	16.3	15.6	--	0.6
M-7 A1 (e)	2.4	1.7	16.1	67.2	1.2	--	--	7.4	2.0	0.5	--	1.6	--	--
M-7 A2 (e)	1.7	2.7	7.7	32.1	3.0	--	0.2	4.3	7.2	5.9	28.8	6.4	--	--
M-7 A3 (e)	0.6	2.9	2.7	11.0	7.6	--	0.2	2.5	12.9	5.8	33.6	20.3	--	--
M-9 A1 (f)	1.3	1.7	8.5	74.3	0.6	0.1	0.1	4.1	4.7	0.6	0.3	3.8	--	--
M-9 A2 (f)	1.0	1.3	6.5	46.8	1.2	0.4	0.3	2.0	4.4	1.2	28.0	2.9	2.1	2.0
M-9 A3 (f)	0.7	1.3	6.4	47.0	1.0	0.1	0.2	1.9	3.0	1.7	30.7	2.9	0.7	2.4

Figure 10. Binocular microscope images (a, b, c) and SEM micrographs (d, e, f). a) Surface brown aggregates from glass sample M-10. b) Interlaminated dark deposits from glass sample M-7. c) Iridescent layers and dark deposits from glass sample M-9. d) Surface brown aggregates from glass sample M-10. e) Interlaminated dark deposits from glass sample M-7. f) Iridescent layers and dark deposits from glass sample M-9. The table attached shows average results from EDS microanalyses (wt %). -- Not detected.

In all the cases the crater surface presented a light dealkalinization (Fig. 8, tab. attached). Likewise, surface dealkalinization layers were observed in all the glass samples. Most of these layers appeared fractured and showed different interference colours due to the optical effect of light diffraction on superimposed layers (Fig. 9a). In general, these dealkalinization layers appeared parallel to the glass surface (Fig. 9a and c), even though a continuous pit network on the iridescent layer of sample M-6 was also observed (Fig. 9b).

As far as deposits are concerned, two different types were identified: surface brown aggregates and interlaminated dark deposits. The former were only located in the sample M-10. The brown aggregates appeared as circular isolated deposits of ~20 μm in diameter, which showed a unique layer when they grow (Fig. 10a, d). Such deposits presented high contents of iron and manganese oxides (Fig. 10d, analysis M-10 A2 and A3). The iridescent layer which lies under those deposits also presented a relatively high percentage of these oxides (Fig. 10d, analysis M-10 A1).

The samples M-3, M-7, M-9, M-11, M-12, and M-13 presented interlaminated dark deposits. These deposits were observed either on the surface (Fig. 10b) or between the iridescent layers (Fig. 10c). They are formed by interconnected spherical deposits of ~2 μm in diameter. The analysis of deposits and the most external iridescent layers detected high concentrations of manganese and iron oxides (Fig. 10e, analysis M-7 A2 and A3), while a low concentration of iron oxide was determined on the surface (Fig. 10e, analysis M-7 A1). Dark deposits located between dealkalinization layers up to ~125 μm in depth were observed in a cross-section of the sample M-9 (Fig. 10c, f). Analyses of these deposits demonstrated that the content of the manganese oxide was close to 30 wt % and the concentration of iron oxide was 2.9 wt % (Fig. 10f, analysis M-9 A2 and A3). However, in the adjacent layers the content of MnO was lower than 0.5 wt % and the concentration of Fe_2O_3 was ~4 wt % (Fig. 10f, analysis M-9 A1). A percentage of lead oxide close to 2 wt % was also detected in the internal deposits. This oxide was not detected by XRF in the bulk of this sample.

Craters and dealkalinization layers are present in all the samples, independently of site and chronology. These pathologies are related with the archaeological degradation. The humidity present in the soil may react with the glass surface leaching out the alkaline oxides of sodium and potassium and give rise to a thin hydrated layer. Repeated cycles of rain/drought can increase the number of layers, thereby decreasing the thickness of the glass fragment.

In contrast, brown aggregates are present only in one sample (M-10), which is a melt waste from the fourth century AD. This sample has the highest content of MnO and Fe_2O_3. Interlaminated dark deposits are present in one sample of flat glass from the Early Empire (sample M-3) and in five fragments from Late Roman times (M-7, M-9, M-11, M-12 and M-13). Sample M-3 displays small isolated deposits, while the Late Roman fragments present nearby deposits or homogeneous layers. The presence of these deposits in samples from different places dated from the fourth century AD onward indicates that they are related, in all probability, with the composition of Late Roman glasses.

4. DISCUSSION

From the compositional point of view all the samples can be classified as natron-based soda lime silicate glasses. All of them showed a very stable sulphur dioxide to chlorine ratio, which could likewise indicate for a single source of natron as alkaline supply (Tab. II). However, glass samples can be separated into two groups. A first one composed of Early Empire glass

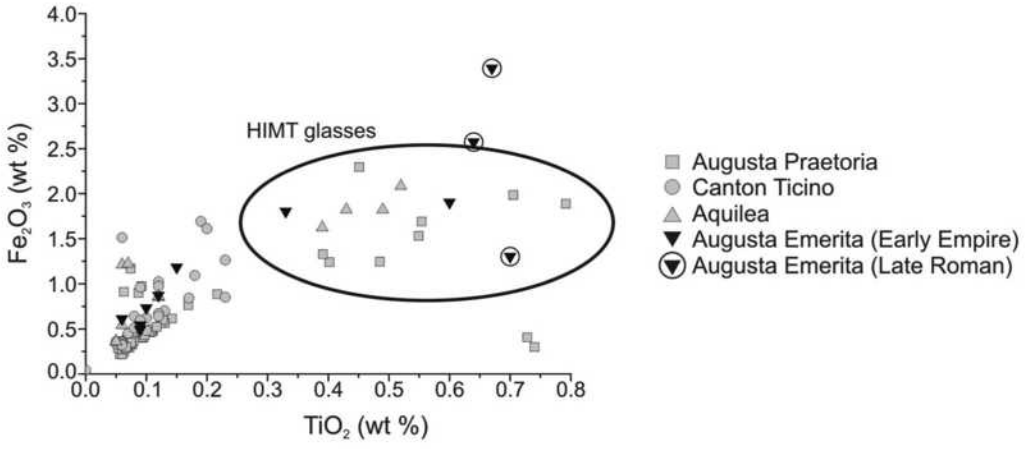

Figure 11. Binary plot of TiO_2 vs. Fe_2O_3 (wt %) contents for the analyzed glasses and those taken from the literature. After Fig. 4 by Arletti *et al.* (2008), modify by the authors.

samples M-1 to M-9, and a second one composed of glass samples M-10 to M-13 from the fourth century AD onward (see Liritzis *et al.*, 1997)

Compared with other coeval glasses reported in the literature (e.g., Mirti *et al.*, 1993, Arletti *et al.*, 2008), the first group showed consistent similarities with Early Empire examples from other western European locales (Fig. 11). This fact could suggest, on the one hand, that Augusta Emerita received the same type of glasses than other contemporary cities of the Empire, such as Augusta Praetoria and Aquilea (Italy) or Canton Ticino (Switzerland); and on the other hand, that glass was elaborated, at much, within a secondary production scale, since only one melt waste (sample M-9) is represented among the glasses here analyzed. On the contrary, those glasses from the fourth century AD onward must be classified into the frame of HIMT glasses, which are characterized by high iron, manganese, and titanium contents (Fig. 11). HIMT glasses were first recognized by Freestone (1994) in raw chunks from Carthage, and later identified as a widely traded glass recovered at many sites in the western region of the Empire. This glass is typically pale green to olive in colour. It is common in Italy and has been found as far away as Britain (Foy *et al.*, 2000, Freestone *et al.*, 2002, 2005, Mirti *et al.*, 1993, Arletti *et al.*, 2005). The presence of this group of glasses likewise indicate that Augusta Emerita was still receiving glass types similar to those found in other western locales from the fourth century AD. Two of the four HIMT glasses from Augusta Emerita are melt wastes, which could also suggest that glass was not produced from local raw materials but imported as raw chunks and later re-melted and worked in secondary local workshops. In addition, two samples (M-1 and M-7) dated in Early Imperial times lay within the area of HIMT glasses taken from the literature (Arletti *et al.*, 2008). The sample M-1 showed a relatively low content of TiO_2 (0.33 wt %) and perhaps it might not be strictly considered as a HIMT glass. The sample M-7 came from a dump context and, consequently, it could be dated later. In any case, chemical data from the M-7 sample were determined by EDS, which may introduce some uncertainty in terms of comparison with the rest of the samples. Finally, the data from the sample M-13 was

not plotted in Fig. 11 since titanium oxide was not detected in the EDS analysis. Nevertheless, in all probability, it deals also with a HIMT glass.

Early Empire glasses of the first group presented a quite homogeneous chemical composition near to 66 wt % of SiO_2, 17 wt % of [Na_2O + K_2O], and 12 wt % of [MgO + CaO + Al_2O_3]. It deals, therefore, with a kind of glass which has a compact network and quite stable against chemical degradation. Surface pathologies observed in these glasses can be associated to its chemical stability, since they only showed craters and surface alterations consisting of dealkalinized layers. Only the M-3 glass fragment presented small isolated black deposits over iridescent layers. On the other hand, glasses from the fourth century AD onward displayed a more dispersed chemical composition characterized by a lower content of SiO_2, a higher content of Na_2O, as well as a relatively high concentration of iron, manganese, and titanium oxides. The result of such a composition is a glass with a more open network, which favours the entrance of water and other weathering compounds. These factors enhance the extraction and leaching of alkaline oxides. All the glasses of this group with Na_2O contents higher than 16 wt % showed interlaminated dark deposits. Furthermore, those samples with the highest Na_2O content (M-12 and M-13) presented the most abundant and homogeneously distributed interlaminated dark deposits on their surfaces.

The high content of manganese and iron oxides together with the chemical instability of this glass, which is due to the high percentage of alkaline oxides, could be the reason why dark deposits were formed on the surface and between the most external iridescent layers. Such deposits could be originated by precipitation of MnO_2 in micro-cracks located between these iridescent layers. Those deposits closer to the surface showed high contents of both iron and manganese oxides, while manganese oxide and a low concentration of lead oxide were detected in the most internal layers. The morphology and physical characteristics of the precipitated MnO_2 allow the physical adsorption of other metallic ions (McKenzie, 1980). This particular feature favoured that the most internal deposits were enriched in those ions lixiviated from the glass, while deposits closer to the surface were enriched in those ions brought by the ground water.

5. CONCLUSIONS

The archaeometric characterization of a representative set of glass samples has provided, for the first time, some insights on composition and technology of glasses found in the Roman town of Augusta Emerita (Mérida, Spain). Compositional data showed that all the samples can be classified as natron-based soda lime silicate glass. However, they can be separated into two groups: one composed of Early Empire glasses and a second one composed of Late Roman glasses from the fourth century AD onward, which is characterized by the presence of the so-called HIMT (high iron, manganese, and titanium) glasses.

The comparison of these two groups with other coeval glasses reported in the literature, either from the Iberian Peninsula or from other locations of the western region of the Empire, suggests that Augusta Emerita roughly received the same type of glasses from Early Imperial to Late Roman times. The only evidence recovered up to now connected with glass production, which mainly concerns with probable blow canes and melt wastes finds from the town widening site, strongly suggests that Augusta Emerita glasses were probably elaborated within the frame of a secondary production scale rather than produced in primary workshops with local raw materials.

The glass samples studied showed different coloration. The iron oxide was

present in all the glasses. In those samples with low contents the iron oxide can be attributed to sand source impurities, while in those ones with higher contents it can be attributed to other kind of raw materials or even being the result of recycling. Three flat glass samples, which probably were window glasses, exhibited a higher content of manganese oxide with respect to the content of iron oxide, which could indicate the intentional addition of MnO_2 as a glass decolouring agent. The main chromophore of an emerald green glass was copper (Cu^{2+}), which was probably incorporated into the glass through the addition of bronze shavings.

Finally, as far as the state of preservation and degradation pathologies of glasses are concerned, some outstanding differences connected to composition and chronology were found, since Late Roman glass samples presented a higher and distinct degree of alteration than Early Empire ones. Thus, while Early Empire glasses only showed surface alterations consisting on craters and dealkalinized layers, those from the fourth century AD onward presented, moreover, surface brown aggregates and interlaminated dark deposits. These distinct pathologies are connected with the different composition and structure of the two kinds of glasses. The Early Empire glass has a more compact and stable chemical structure, which slows down its chemical degradation, while Late Empire glasses present a more open and weak chemical structure, which favours the leaching of alkaline oxides and speeds up its corrosion.

ACKNOWLEDGEMENTS

The authors acknowledge to the National Museum of Roman Art (Mérida, Spain) and, especially, to its director Dr J.M. Álvarez Martínez, the facilities provided to accomplish this research. They also acknowledge partial funding of the programs Consolider Ingenio 2010 Ref. TCP CSD2007-00058 and Geomateriales Ref. S2009/Mat-1629, as well as professional support from Techno-Heritage (Network of Science and Technology for Heritage Conservation). T. Palomar acknowledges a pre-doctoral grant from the Spanish Ministry of Science and Innovation (MICINN).

REFERENCES

Allen, D. (1998) *Roman Glass in Britain,* Shire Publications, Princes Risborough, Buckinghamshire.

Arletti, R., Giordani, N. Tarpini, R. and Vezzalini, G. (2005) Archaeometrical analysis of ancient glass from western Emilia Romagna (Italy) belonging to the Imperian Age, in *Annales du 16e Congrès de l'Association Internationale pour l'Histoire du Verre,* 80-84, AIHV, Nottingham.

Arletti, R., Vezzalini, G., Biaggio Simona, S. and Maselli Scotti, F. (2008) Archaeometrical studies of Roman Imperial Age glass from Canton Ticino. *Archaeometry*, vol. 50, No 4, 606-626.

Caballero Zoreda, L. and Ulbert, T. (1976) *La basílica paleocristiana de Casa Herrera en las cercanías de Mérida (Badajoz),* Excavaciones Arqueológicas en España. Ministerio de Educación y Ciencia, Madrid.

Caldera de Castro, M.P. (1983). El vidrio romano emeritense. *In Augusta Emerita I. Excavaciones arqueológicas en España*, Ministerio de Cultura. Dirección General de Bellas Artes y Archivos, Madrid.

Carmona, N., Villegas, M.Á., Castellanos, M.A., Montero Ruiz, I. and García-Heras, M.

(2008). Análisis de vidrios romanos del yacimiento de la Dehesa de la Oliva (Patones, Madrid). In *Actas VII Congreso Ibérico de Arqueometría (Madrid, 8-10 octubre 2007)*, Madrid.

Carmona, N., Villegas, M.A., Jiménez, P., Navarro, J. and García-Heras, M. (2009) Islamic glasses from Al-Andalus. Characterisation of materials from a Murcian workshop (12th century AD, Spain). *Journal of Cultural Heritage*, vol. 10, No 3, 439-445.

Domenech-Carbo, M.T., Domenech-Carbo, A., Osete-Cortina, L. and Sauri-Peris, M.C. (2006) A study on corrosion processes of archaeological glass from the Valencian Region (Spain) and its consolidation treatment. *Microchimica Acta*, vol. 154, No 1-2, 123-142.

Dominguez-Bella, S. and Jurado-Fresnadillo, G. (2004) Análisis arqueométrico de los vidrios romanos de la Casa del Obispo (Cádiz). *Avances en Arqueometría: 2003*, 129-137.

Férnandez Navarro, J.M. (2003) *El vidrio*, 3rd. edition, Consejo Superior de Investigaciones Científicas, Madrid.

Fleming, S.J. (1999) *Roman Glass: Reflections on Cultural Change*, University of Pennsylvania. Museum of Archaeology and Anthropology, Philadelphia.

Foy, D., Vichy, M. and Picon, M. (2000) Lingots de verre en Méditerranée occidentale, in *Annales du 14e Congrès de l'Association Internationale pour l'Histoire du Verre*, 51-57, AIHV, Amsterdam.

Freestone, I.C. (1994) Chemical analysis of 'raw' glass fragments, in Excavations at Crathage, volume II, The Circular Harbour, north side (ed. H.R. Hurst), 290, Oxford University Press for the British Academy, Oxford.

Freestone, I.C. (2005) The provenance of ancient glass through compositional analysis. *In Materials Issues in Art and Archaeology VII*, Boston.

Freestone, I.C. (2006) *Glass production in Late Antiquity and the Early Islamic period: a geochemical perspective*, Geological Society of London. Special Publications, London.

Freestone, I.C., Ponting, M. and Hughes, M.J. (2002) The origins of Byzantine glass from Maroni Petrera, Cyprus. *Archaeometry*, vol. 44, No 2, 257-272.

Freestone, I.C., Wolf, S. and Thirlwall, M. (2005) The production of HIMT glass: elemental and isotopic evidence, in *Annales du 16e Congrès de l'Association Internationale pour l'Histoire du Verre*, 153-157, AIHV, Nottingham.

Garcia-Heras, M., Sánchez de Prado, M.D., Carmona, N., Tendero, M., Ronda, A.M. and Villegas, M.A. (2007) Analytical study of Roman glasses from Southeastern Spain. *Archaeologia Polona*, vol. 45, 63-78.

García Sandoval, E. (1966) *Informe sobre las casas romanas de Mérida y excavaciones en la "Casa del Anfiteatro"*, Excavaciones arqueológicas en España. Ministerio de Educación y Ciencia, Madrid.

Gómez-Tubío, B., Ontalba Salamanca, M.Á., Ortega-Feliu, I., Respaldiza, M.Á., Amores Carredano, F. and González-Acuña, D. (2006) PIXE-PIGE analysis of late roman glass fragments. *Nuclear Instruments and Methods in Physics Research Section B: Beam Interactions with Materials and Atoms*, vol. 249, No 1-2, 616-621.

Isings, C. (1957) *Roman glass from dated finds*, Archaeologica Traiectina, Groningen and Djakarta.

Jackson, C.M., Cool, H.E.M. and Wager, E.C.W. (1998) The manufacture of glass in Roman York. *Journal of Glass Studies*, vol. 40, 55-61.

Lang, J. and Price, J. (1975) Iron Tubes from a Late Roman Glassmaking site at Mérida

(Badajoz), in Spain. *Journal of Archaeological Science,* vol. 2, No 4, 289-296.

Liritzis Y., Salter C. and Hatcher H. (1997) Chemical Composition of some Greco-Roman glass fragments from Patras, Greece. *European journal of PACT,* No 45, I2, 25-34

McKenzie, R.M. (1980) The adsorption of lead and other heavy metals on oxides of manganese and iron. *Australian Journal of Soil Research,* vol. 18, No 1, 61-73.

Mirti, P., Casoli, A. and Appolonia, L. (1993) Scientific analysis of Roman glass from Augusta Praetoria. *Archaeometry*, Vol. 35, No 2, 225-240.

Paynter, S. (2006) Analyses of colourless Roman glass from Binchester, County Durham. *Journal of Archaeological Science,* vol. 33, No 8, 1037-1057.

Ramón Peris, M.A. (2002-2003) Estudio del vidrio hallado en la villa rústica romana de l'Hort de Pepica (Catarroja, Valencia). *Quaderns de prehistòria i arqueologia de Castelló,* vol. 23, 261-286.

Rincón, J.M. (1984) Análisis y microestructura de vidrios romanos de Mérida y Segóbriga. *Revista de Arqueología,* vol. 43, 34-39.

Silvestri, A., Molin, G. and Salviulo, G. (2005) Roman and Medieval glass from the Italian area: Bulk characterization and relationships with production technologies. *Archaeometry*, vol. 47, No 4, 797-816.

Stern, E.M. (1999) Roman glassblowing in a cultural context. *American Journal of Archaeology,* vol. 103, No 3, 441-484.

Vigil Pascual, M. (1969) *El vidrio en el mundo antiguo,* Instituto Español de Arqueología. Consejo Superior de Investigaciones Científicas, Madrid.

Wedepohl, K.H. and Baumann, A. (2000) The use of marine molluscan shells for Roman glass and local raw glass production in the Eifel area (western Germany). *Naturwissenschaften*, vol. 87, 129-132.